Electronic Supplementary Information (ESI) for

Nanorod bundle-like silver cyanamide nanoparticles for high-efficiency photocatalytic degradation of tetracycline

Yulin Li, Chencong Cao, Qing Zhang, Ying Lu, Yanxi Zhao, Qin Li, Xianghong Li, Tao Huang*

Key Laboratory of Catalysis and Energy Materials Chemistry of Ministry of Education, College of Chemistry and Materials Science, South-central University for Nationalities, Wuhan 430074, China

*Correspondence E-mail: huangt208@163.com

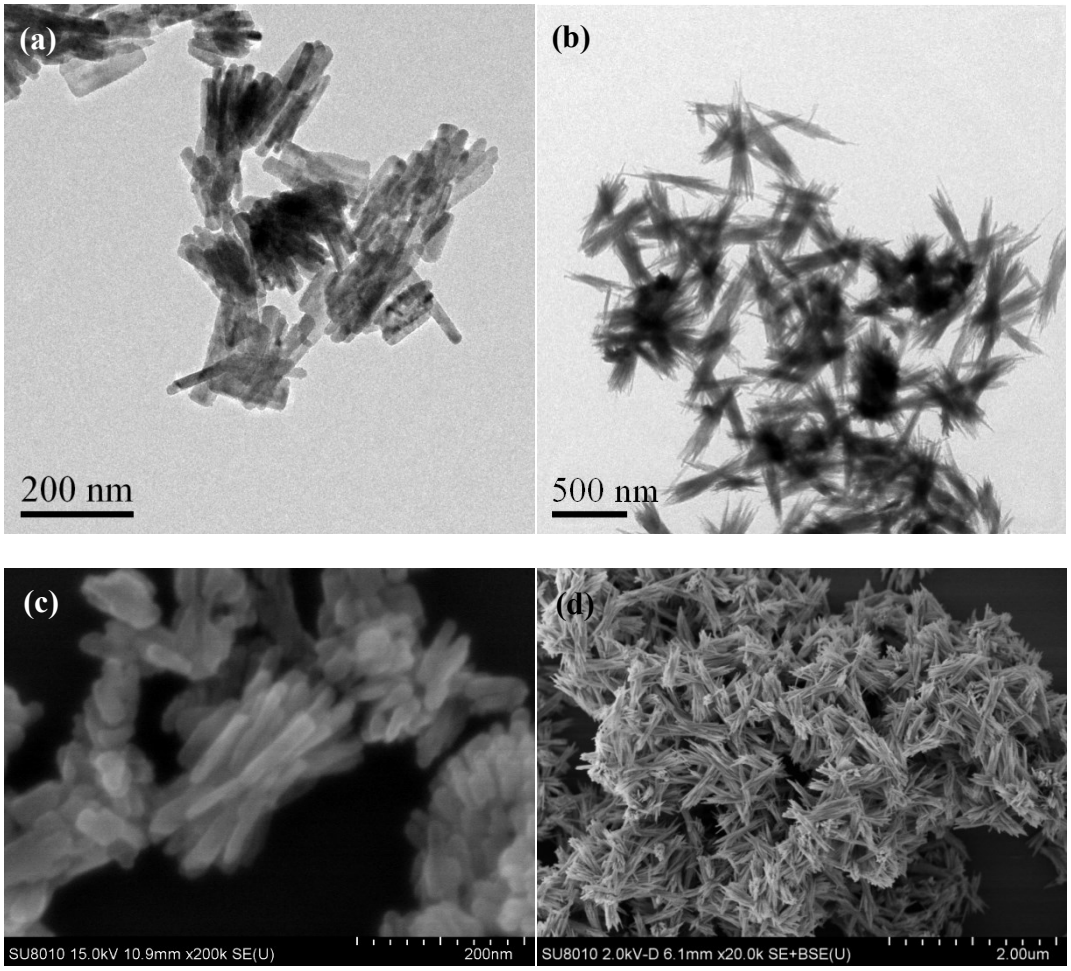

Figure S1 TEM and SEM images of RB and SB samples. (a) TEM image of RB samples; (b) TEM image of SB samples; (c) SEM image of RB samples; (d) SEM image of SB samples.

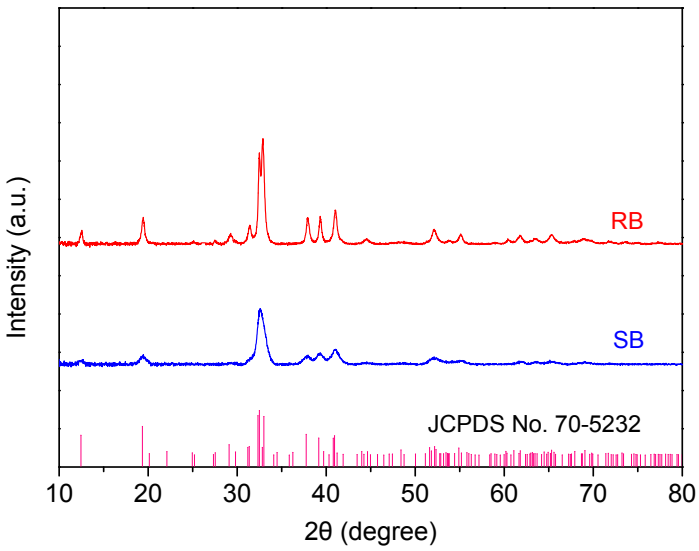

Figure S2 XRD patterns of SB an RB samples.

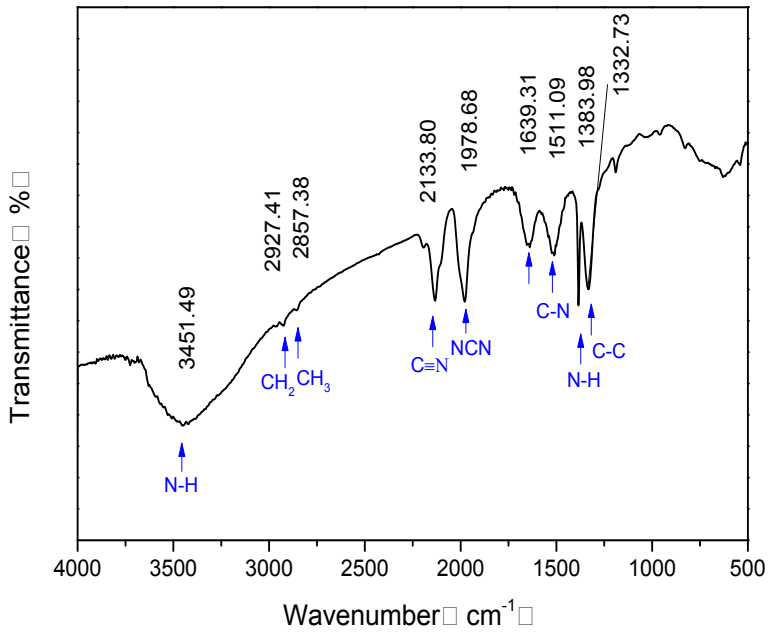

Figure S3 The FT-IR spectra of RB samples.

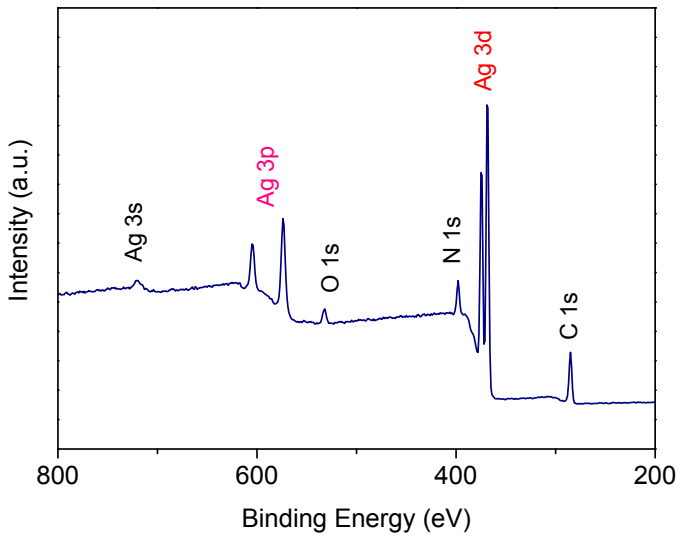

Figure S4 The full-scale XPS spectra of RB samples.

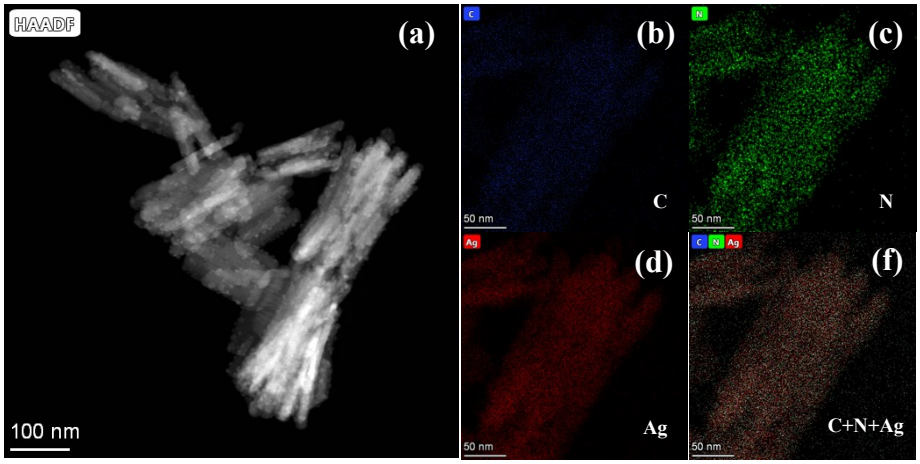

Figure S5 EDS mapping analyses for RB samples. (a) HAAADF image; (b) C; (c) N; (d) Ag; (f) C+N+Ag.

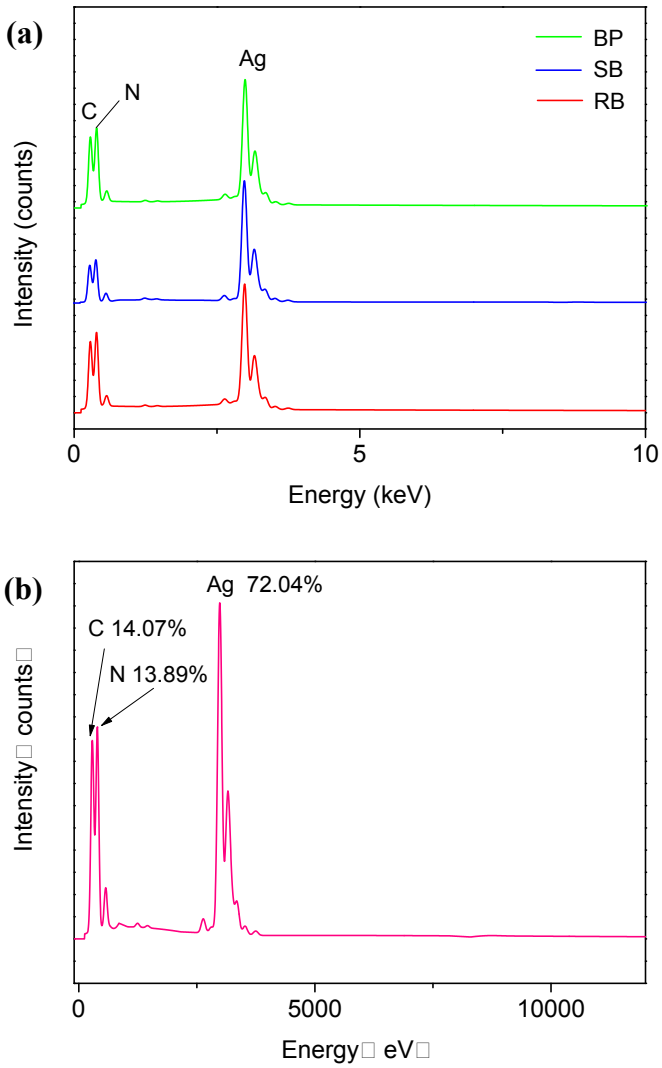

Figure S6 EDS spot analyses. (a) RB, SB and BP samples; (b) RB samples.

Table S1 Elemental contents in RB and SB samples obtained by EDS spot analyses

Sample	Ag	C	N
Normal Ratio (wt%)	84.35	4.70	10.95
RB	72.04	14.07	13.89
SB	81.28	8.86	9.86
BP	86.54	5.93	7.54

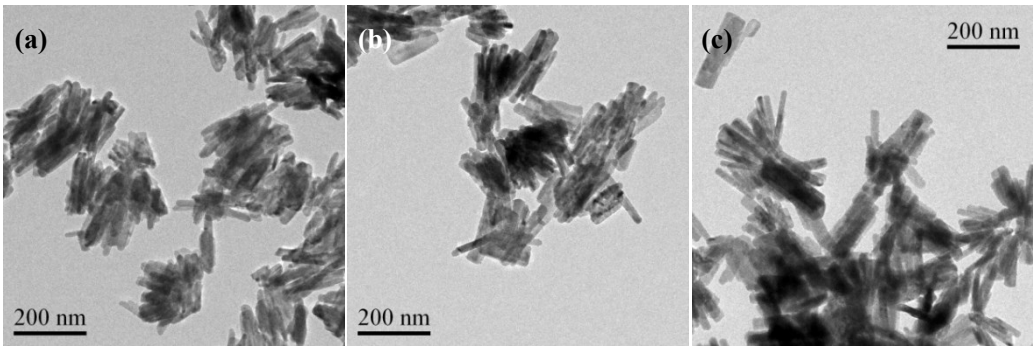

Figure S7 TEM images of Ag_2NCN nanocrystals prepared in n-octylamine system at different temperatures. (a) 0 °C; (b) 25 °C; (c) 60 °C.

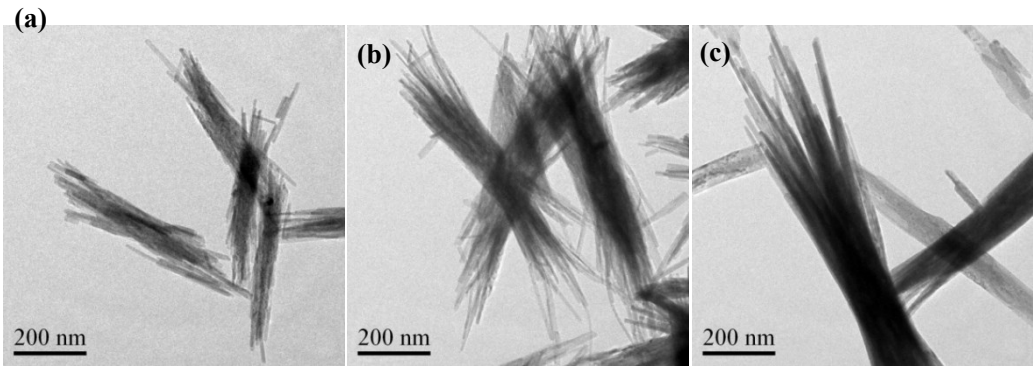

Figure S8 TEM images of Ag_2NCN nanocrystals prepared in t-butylamine system at different temperatures. (a) 0 °C; (b) 25 °C; (c) 60 °C.

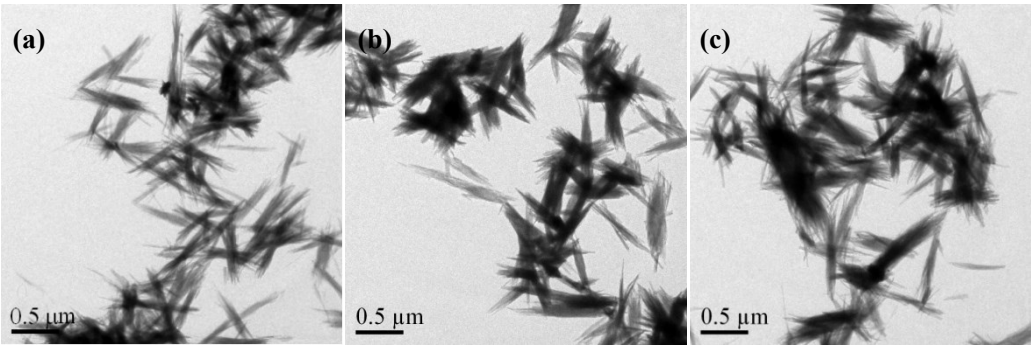

Figure S9 TEM images of Ag_2NCN nanocrystals prepared in t-butylamine system at different times. (a) 30 min; (b) 1 h; (c) 2 h.

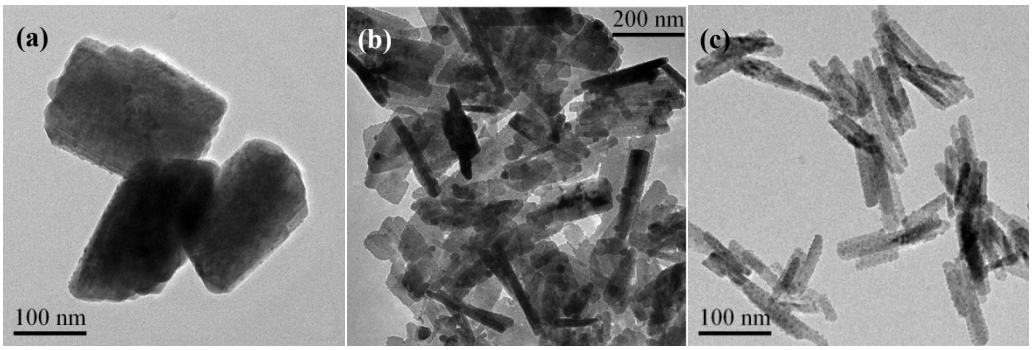

Figure S10 TEM images of Ag_2NCN nanocrystals obtained with using ethylamine (a), n-butylamine (b) or oleylamine (c).

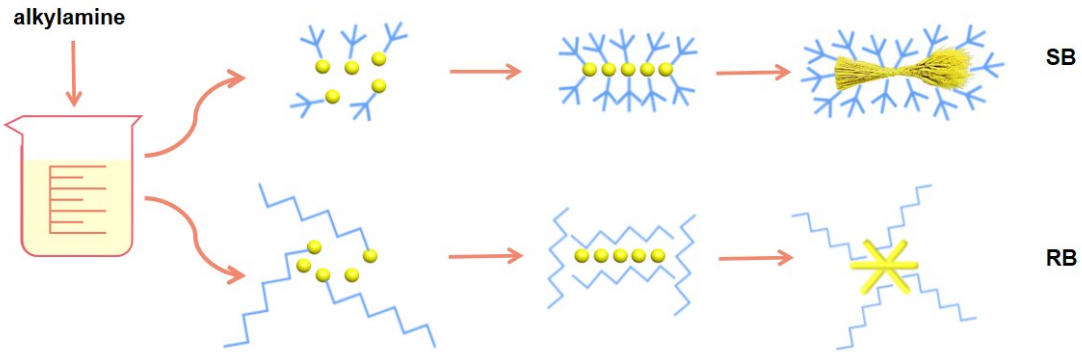

Figure S11 Scheme illustration for the growth process of SB and RB nanostructures.

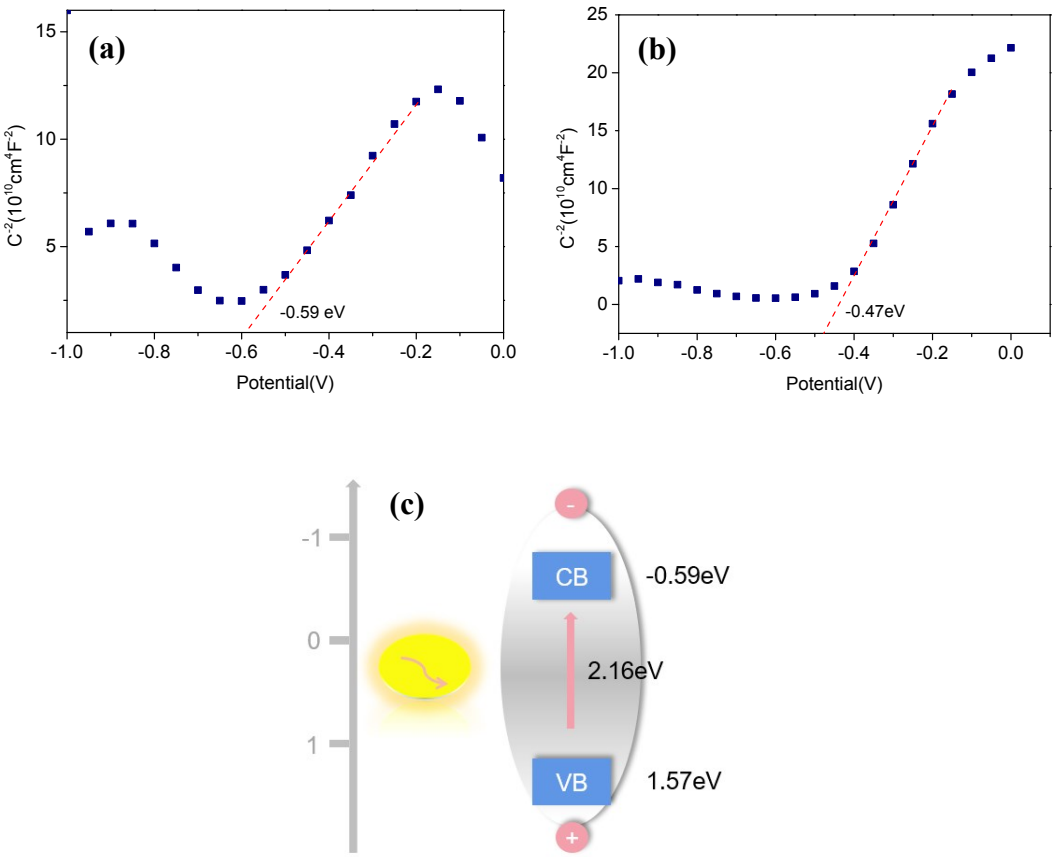

Figure S12 (a) and (b) Mott-Schottky plots of RB and SB samples; (c) The band structure diagram of RB.

Table S2 The energy band structures of te asprard Ag_2NCN naoparticles

Samples	Eg/eV	E_{CB}/V	E_{VB}/V
RB	2.16	-0.59	1.57
SB	2.24	-0.47	1.77

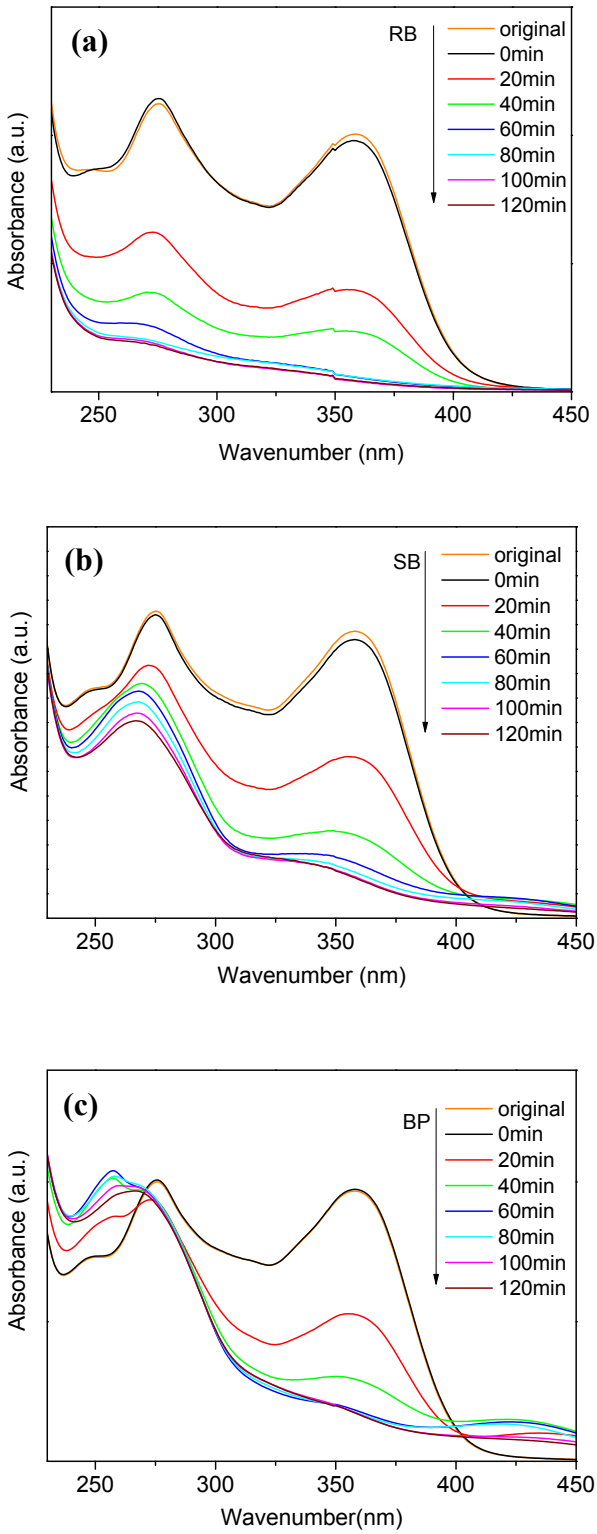

Figure S13 UV-vis adsorption spectra of TC in photocatalytic degradation process in 120 min over RB samples (a), SB samples (b) and BP samples (c)

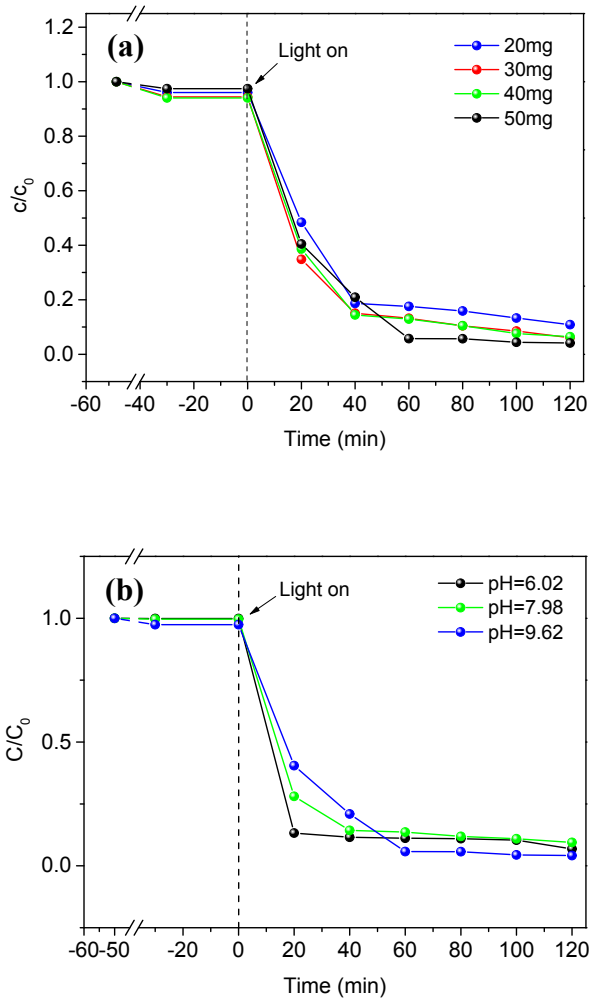

Figure S14 (a) The effect of the catalyst dosage on the photocatalytic degradation process; (b) The effects of pH values on the photocatalytic degradation process.

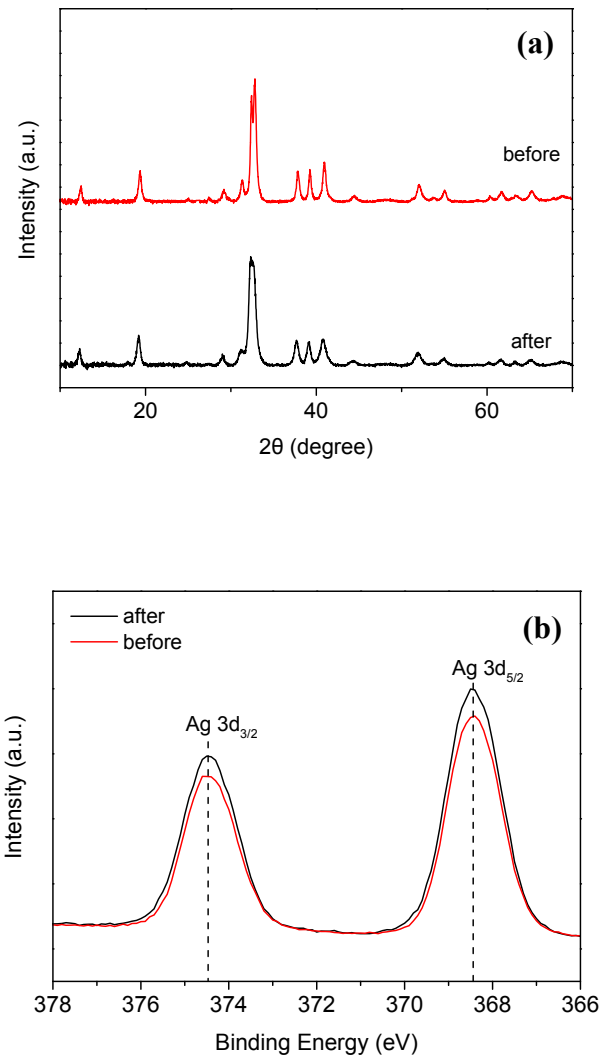

Figure S15 XRD pattern (a) and XPS spectra (b) of RB samples after four cycles.

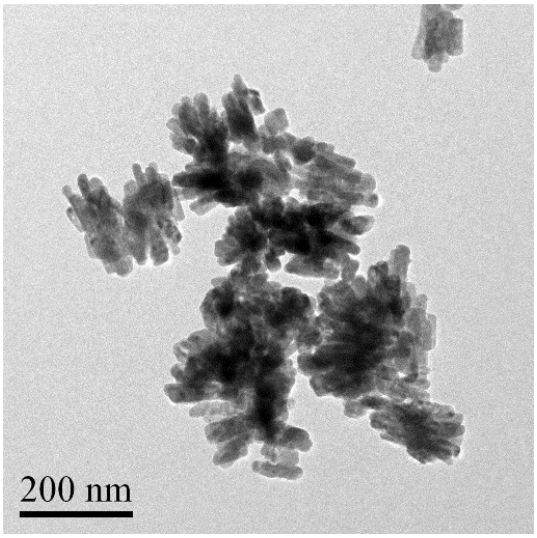

Figure S16 TEM images of RB samples after four cycles.

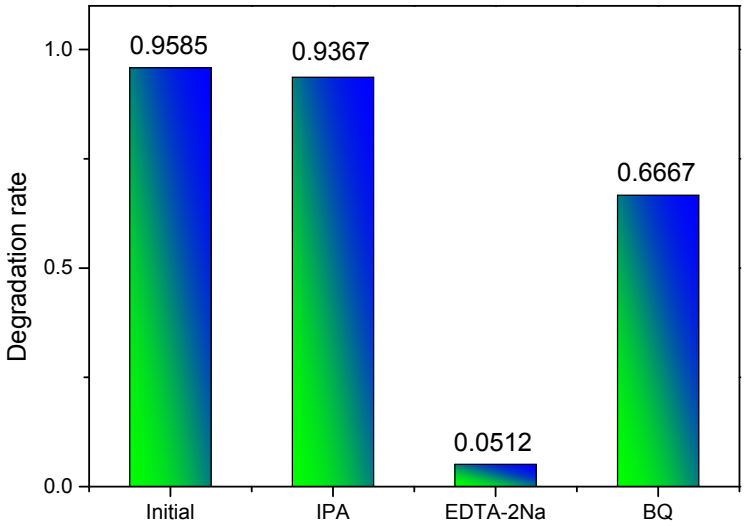

Figure S17 The degradation rate of TC over RB samples with different quenchers.

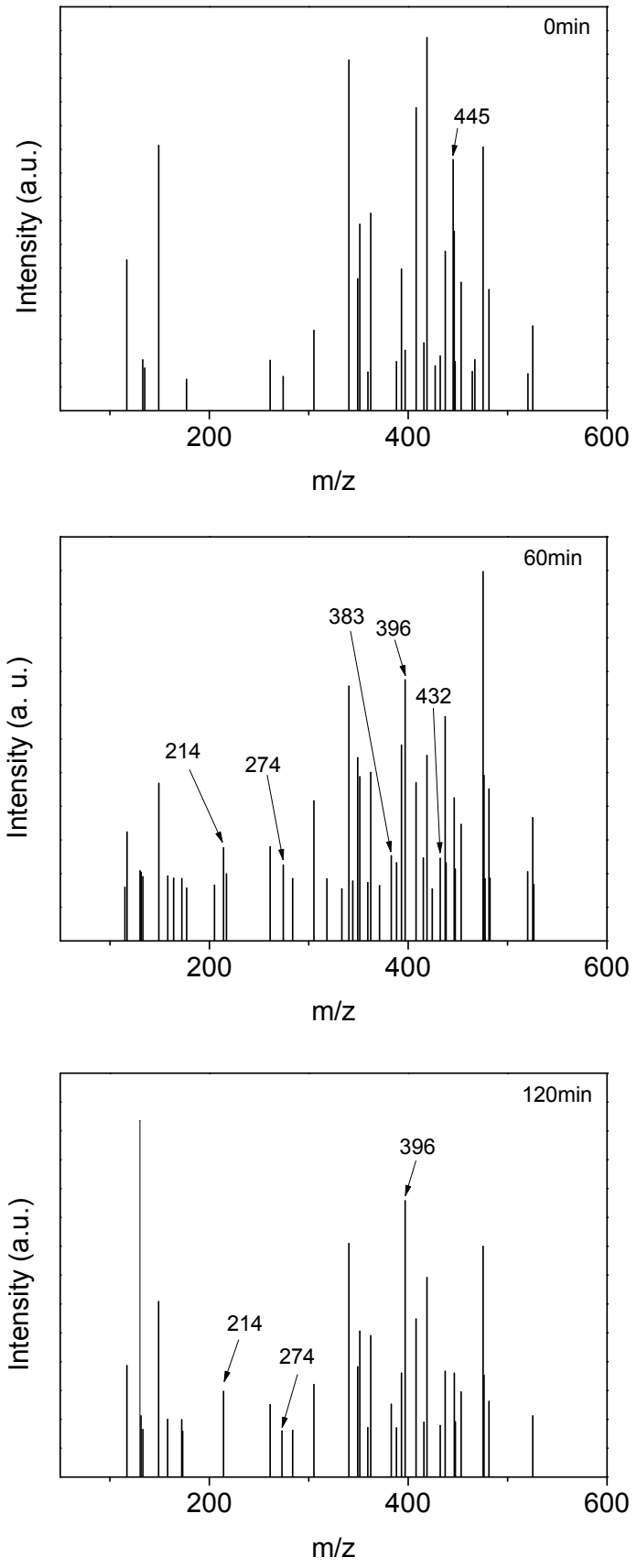

Figure S18 HPLC-MS spectrograms for the intermediate products at different

degradation time.

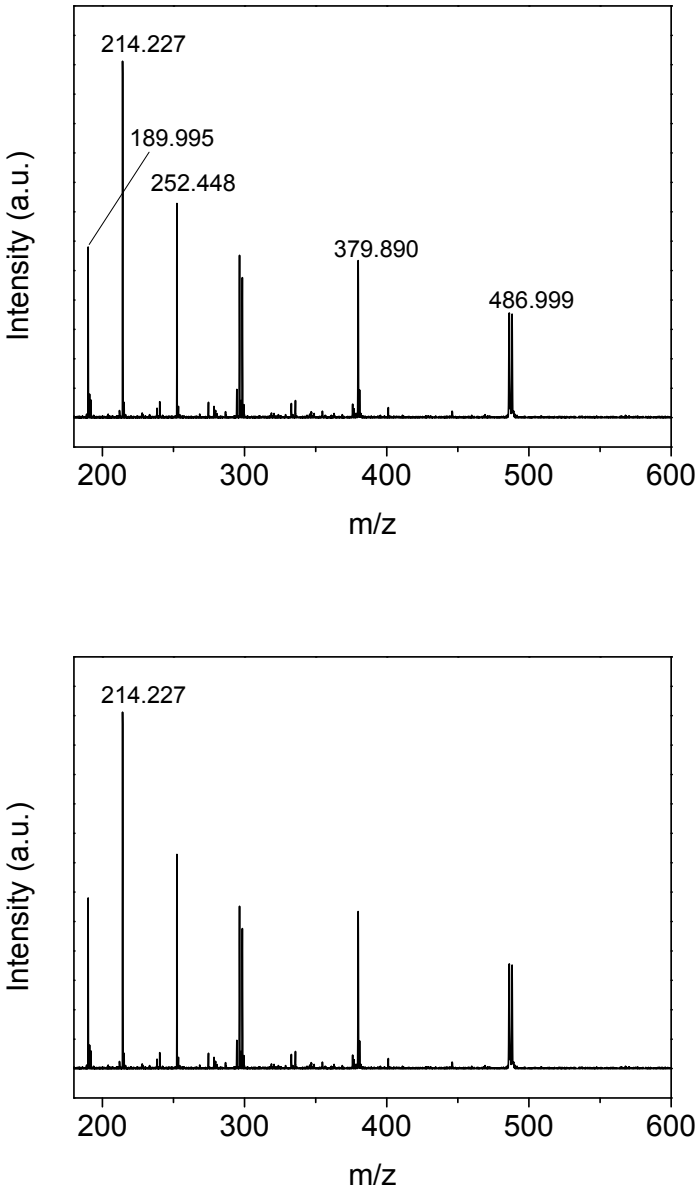

Figure S19 MALDI-TOF-MS spectrograms for the intermediate products in 120-min degadation.

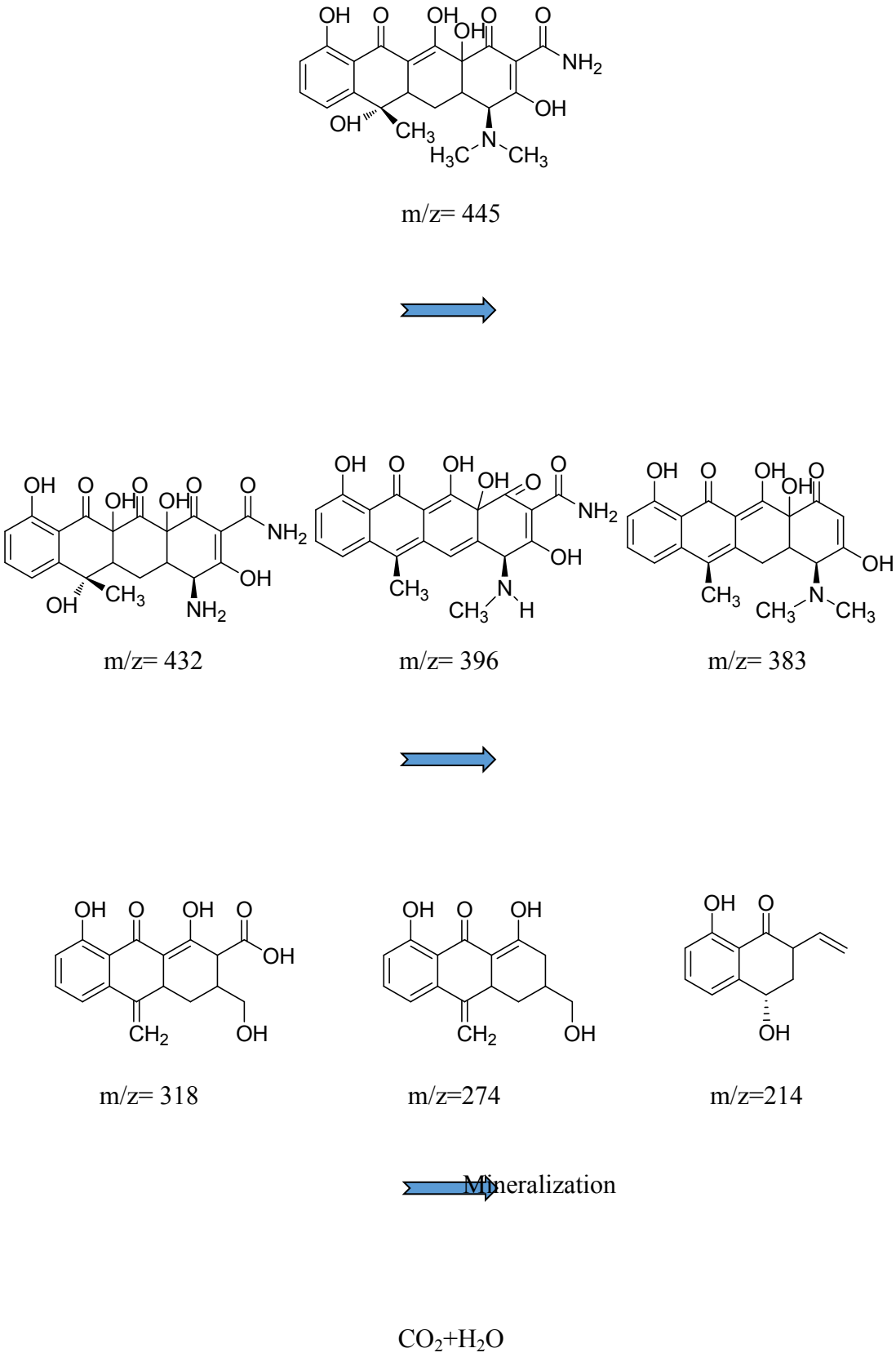

Figure S20 The possible pathway for the photocatalytic degradation of TC.